

FINAL PUBLISHABLE REPORT

Grant Agreement number 15HLT08
 Project short name MRgRT
 Project full title Metrology for MR guided Radiotherapy

Project start date and duration:		01 June 2016, 36 months
Coordinator: Jacco de Pooter, VSL Tel: +31-15 269 1623		E-mail: jdpooter@vsl.nl
Project website address: http://www.mrgrtmetrology.nl/		
Internal Funded Partners:	External Funded Partners:	Unfunded Partners:
1. VSL, The Netherlands	5. DKFZ, Germany	8. Christie, United Kingdom
2. CEA, France	6. UoM, United Kingdom	9. METAS, Switzerland
3. NPL, United Kingdom	7. UMCU, The Netherlands	
4. PTB, Germany		
RMG: -		

TABLE OF CONTENTS

1	Overview	3
2	Need	3
3	Objectives	3
4	Results	4
4.1	A metrological framework (primary and secondary standards) for traceable dosimetry under reference conditions for MRgRT.....	4
4.2	Measurement of treatment planning system (TPS) input data for MRgRT	9
4.3	Accuracy of the Monte Carlo based radiation transport in magnetic fields	15
4.4	Evaluation of MR based dose delivery under static and dynamic conditions	19
5	Impact	25
6	List of publications.....	27
7	Contact details	28

1 Overview

Cancer patients are treated with radiotherapy in which megavolt (MV) photon beams are used to deliver a high dose of ionizing radiation to target and kill cancerous cells. **MR-guided radiotherapy (MRgRT)**, the simultaneous use of Magnetic Resonance (MR)-imaging and MV photon beams allows clinicians to see what is being treated and to adapt and further optimise the treatment and is next in advanced radiotherapy. The project has improved metrological capabilities in radiation dosimetry and imaging by the investigations and developments on a methodology for reference dosimetry and by the development of quality assurance procedures for clinical MRgRT treatments. This is not only vital for the safe **clinical implementation** of MRgRT but also for future **innovations** in MRgRT.

2 Need

In 2012, cancer incidences in the European Union were approximately 2.6 million people (~0.5 % of the population) per year. The devastating consequences of this disease affected the daily life of a large proportion of the European population with roughly half of these patients being treated using radiotherapy.

In Europe and worldwide several manufacturers and academic hospitals have been developing MR guided radiotherapy facilities. The feasibility of MRgRT was demonstrated by the first successful treatments in 2014. The benefits of MRgRT are:

- an increased accuracy in defining the contours of tumour, organs and other healthy tissue.
- avoidance of additional exposure to harmful radiation from diagnostic imaging modalities (e.g. CT) currently used.
- the ability to image motion, caused by internal movements of the patient (e.g. breathing, swallowing), during treatment. This allows adaptation and optimisation of the dose during the treatment.

The magnetic field cannot easily be switched off for these MR-guided radiotherapy modalities; therefore measurement of the radiation dose (dosimetry) needs to be performed in the presence of the constant magnetic field. Under this condition, both the detectors used for dosimetry and the dose distributions are highly influenced by the magnetic field. Since the underlying physical mechanisms are not well understood, **traceability** for radiation **dosimetry** and adequate **knowledge of detector characteristics** is lacking and no Codes of Practice (**CoP**) are available for reference dosimetry and measurements of the **radiation field characteristics**. Therefore, medical physicists were not able to accurately calibrate the radiation field and characterise the radiation fields in MRgRT for treatment planning. Furthermore, **the accuracy of the Monte Carlo** algorithms required for the calculation of detector response and dose distributions in the presence of magnetic fields needed to be improved further.

To guarantee that the dose distribution is delivered to the patient as intended in treatment planning, the medical physicists and clinicians required Quality Assurance (**QA**) **procedures** and **MR-compatible dynamic phantoms** to verify the dose delivery under static and dynamic conditions, and **methods to determine appropriate safety margins** around the tumour.

3 Objectives

The overall aim of the project was to develop the metrological capacity in dosimetry and imaging required for the safe **clinical implementation and application** of MR guided radiotherapy and to support future **innovations** in MRgRT. The specific scientific and technical objectives of this project were:

1. To develop a metrological framework (primary and secondary standards) for traceable dosimetry under reference conditions for MR guided radiotherapy. This shall include the determination of input data and establishing a formalism for reference dosimetry including reference conditions for future **dosimetry protocols (CoPs)**.
2. To develop methodologies for measurement of treatment planning system (TPS) input data for MRgRT. This should include determination of **detector characteristics** for commercially available detector systems and secondary standards in hybrid fields, and **characterisation of the radiation field** based on measurements and Monte Carlo modelling.

3. To develop methodologies to assess the **accuracy of the Monte Carlo** based radiation transport algorithms in external magnetic fields.
4. To evaluate MR based dose delivery under static and dynamic conditions. This should include:
 - a. determination of associated geometrical uncertainties of standardised MR sequences and accurate registration methods, for the assessment of the overall geometrical uncertainty;
 - b. development of **MR compatible phantoms for quality assurance** of dose distributions for static and dynamic conditions;
 - c. development of reliable MRI target and organ motion tracking methods.
 - d. evaluation of the effect on the residual uncertainties on actual treatment plans **to determine appropriate safety margins** around the tumour.
5. To facilitate the take up of recommendations for dosimetry and MR related quality assurance of MR guided radiotherapy developed by the project by clinicians and industry in order to enable hospitals to perform **quality assurance** based on traceable measurements and support improvements for dosimetry in MRgRT.

4 Results

4.1 A metrological framework (primary and secondary standards) for traceable dosimetry under reference conditions for MRgRT

Relevance

For conventional radiotherapy the metrological framework for traceable dosimetry in a clinical environment is based on primary dosimetry standards such as water calorimeters. Traceability to these standards is disseminated via secondary standards, such as alanine, Fricke dosimetry and ionisation chambers. While the former two are mainly applied by dosimetry laboratories, the latter is also used in hospitals for routine reference dosimetry using the guidelines of accepted codes of practices (CoPs). These CoPs for reference dosimetry generally contain the following elements:

- A clear and concise description of the methodology (formalism) to ensure consistent application of the investigated characteristics and correction factors of the ionisation chambers.
- Ion chamber type specific correction factors to correct for the change in calibration coefficient of the ion chamber between the calibration quality (generally Co-60) and the clinical beam quality.
- Characteristics of ion chambers and methodology to correct for these characteristics

To establish a metrological framework for traceable dosimetry for MRgRT:

- A water calorimeter was developed for application in MRgRT facilities
- the effect of the magnetic field on the response of secondary standards and other characteristics of these standards in magnetic fields were investigated.
- Correction factors for ionisation chambers were determined
- A methodology for reference dosimetry in MRgRT was developed.

A water calorimeter for application in MRgRT facilities

A water calorimeter build by VSL in the previous EMPIR project „HLT06 MRI-Safety“ was further optimized for application in MR-linac facilities. Optimization includes the development of a dedicated beam monitoring system, position measurement system and a tool to rotate ion chambers inside the calorimeter (see Figure 1). In the commissioning process as primary standard all steps in the water calorimeter that can be affected by the magnetic field have been investigated and characterised [1]. The optimized calorimeter was tested and applied by VSL in the first world-wide measurements with a water calorimeter in the presence of a magnetic field. In these measurements the calibration coefficients of a set of ion chambers was determined against the water calorimeter by VSL in an MR-linac of the UMCU. These chambers have been used later on in the preparation of the first clinical treatments with an MR-linac [2]. In a separate measurement reference dosimetry

based on these calibration coefficients has been compared with the alanine system of NPL using a completely independent traceability route. Both methods agree within 0.5% while half of the disagreement can be attributed to the differences in the primary standards of NPL and VSL.

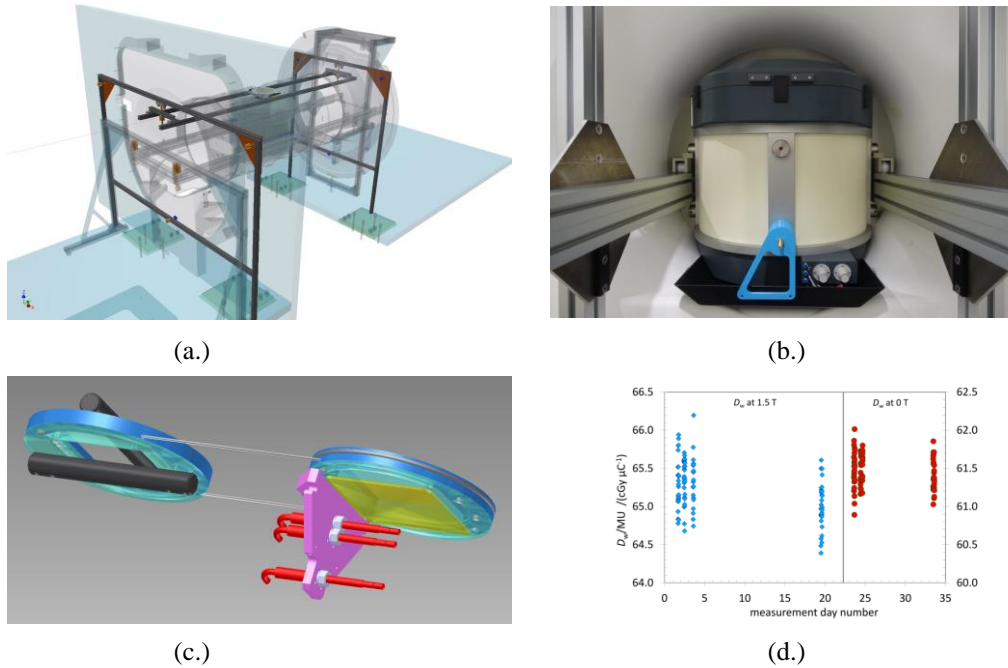


Figure 1. Water calorimetry in MRgRT facilities. (a.) the positioning frame of the VSL water calorimeter in the MR-linac bore. (b.) the water calorimeter in the positioned in the MR-linac bore. (c.) positioning system for ion chambers in the water calorimeter with independent rotation. (d.) Long term results of D_w measured with the water calorimeter in the MR-linac with and without magnetic field present, Reproduced from [1] with permission.

Methodology for reference dosimetry

A formalism for reference dosimetry in MRgRT facilities was developed [3] by UMCU and applied in the preparation of the first clinical treatments of the Elekta Unity system [2]. The new formalism describes how the existing formalisms for reference dosimetry in conventional radiotherapy can be extended to application in MR-linac facilities. The most important aspect of the formalism is the addition of a separate chamber-type specific correction factor, k_B , which corrects for the presence of the magnetic field. k_B is defined as the ratio of calibration coefficients with and without the magnetic field present and depends on the orientation of the ionisation chamber with respect to the magnetic field direction.

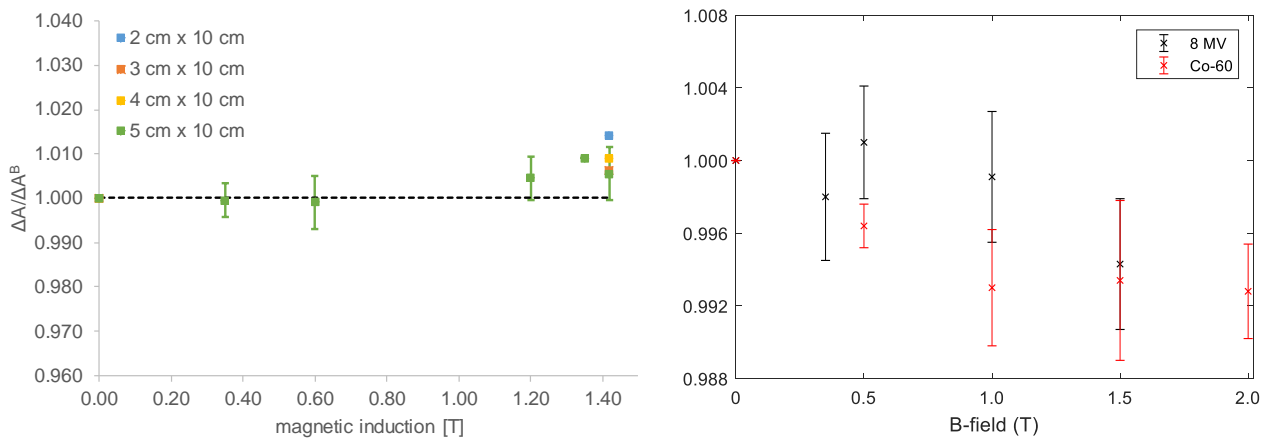


Figure 2 Change in calibration coefficient of alanine (right) and Fricke dosimeters (left) as a function of magnetic field strength.

Characteristics of secondary standards

The characteristics of alanine and secondary standards based on Fricke solutions in the presence of magnetic fields were investigated in this project. It was shown that the calibration coefficient of alanine and Fricke dosimeters is only minor affected by the magnetic field (see Figure 2) by NPL and METAS respectively. For alanine it was shown that this dependency hardly changes with beam quality.

The effect of the magnetic field on saturation and polarity, two commonly known effects in ion chambers, was investigated by VSL [4]. This was done by determining the correction factors for saturation and polarity of two sets of Farmer type ionisation chambers for both effects using commonly applied methods. It was shown that both effects do not significantly differ with and without magnetic field. In addition, the effects were investigated for two different orientations of ionisation chambers and demonstrated to agree.

Table 1 Polarity and recombination factors measured with and without magnetic field present., Reproduced from [4] with permission.

Chamber	beam	B-field	k_s	k_{pol}
PTW 30013	X7	1.5 T	1.0053(5)	1.0000(4)
		0 T	1.0047(1)	1.0002(3)
	^{60}Co	0 T	1.0010(2)	1.0002(3)
IBA FC65-G	X7	1.5 T	1.0060(4)	0.9989(4)
		0 T	1.0054(1)	0.9991(2)
	^{60}Co	0 T	1.0007(2)	0.9991(1)

The dependency on the magnetic field of several characteristics of ion chambers were investigated. It was shown by DKFZ [5] that the dose to the air cavity of ionisation chambers is not homogeneously distributed in the presence of magnetic fields. Part of the ionisation chamber does not contribute to the signal; the so-called dead volume. The dead volume is located in the area of the observed dose inhomogeneities; therefore, this has a considerable impact on how to perform chamber response Monte Carlo simulations in the presence of magnetic fields. Traditionally for these simulations one takes the full volume of the cavity into account. [5] demonstrated that when a specific chosen dead volume is neglected in the Monte Carlo simulations, the simulated response curve matches with measured response curves. However, this was based on the arbitrary assumption of a cylindrical shape of the dead volume.

PTB [6] extended this concept by a more realistic determination of the dead volume by Finite Element Methods (FEM) simulations. They demonstrated that the dead volume for a Farmer type ionisation chamber is not cylindrically shaped, but donut-shaped. Moreover, when taking into account this more realistic dead volume in the Monte Carlo simulations the agreement with measurements is excellent (Figure 3 c.).

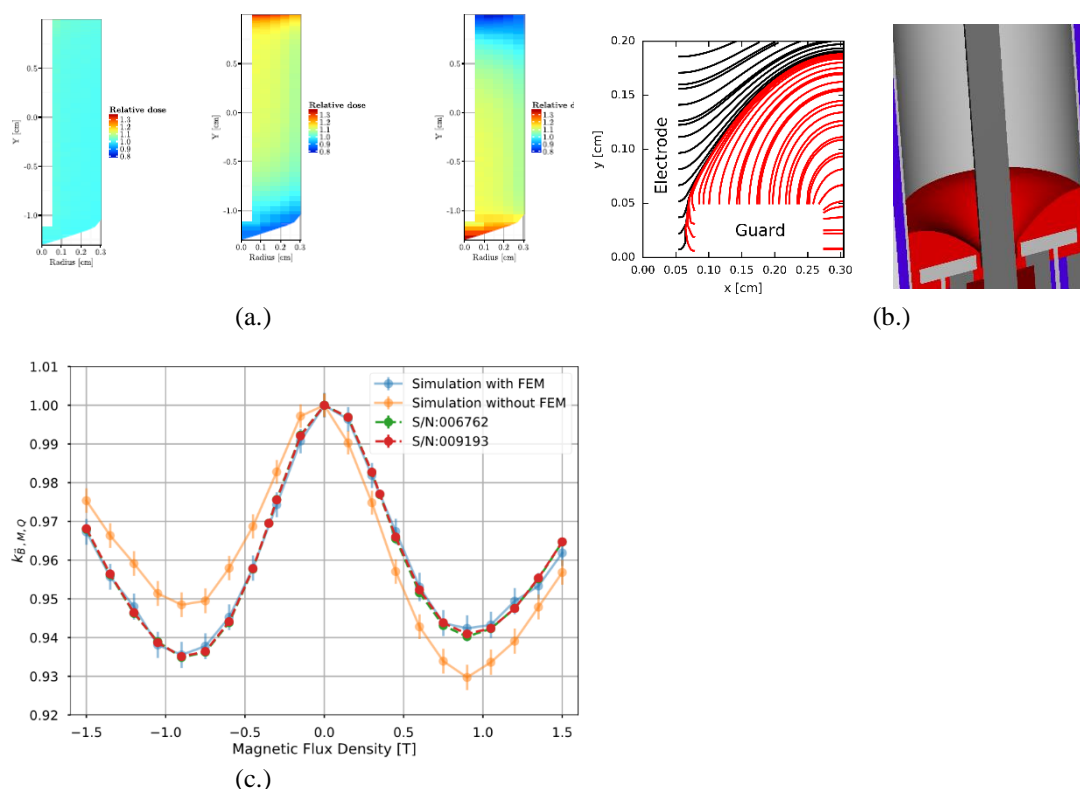


Figure 3 Dead volume effects in magnetic fields. (a) dose distribution in air cavity as a function of magnetic field strength with the chamber axis perpendicular to the magnetic field direction (left; $B = 0.0$ T, middle $B = -1.0$ T and right $B = 1.0$ T). (b) FEM simulation of electrical field lines in a ion chamber cavity. (c) response change simulated in Monte Carlo by scoring the dose to the full cavity and to the cavity excluding the FEM simulated dead volume compared with measurements. , Reproduced from [6] with permission.

Type specific correction factors for ionisation chambers

The developed formalism for reference dosimetry in MRgRT requires an additional chamber specific correction factor, k_B , which corrects for the change in calibration coefficient due to the magnetic field. This correction factor, k_B , is defined as the ratio of calibration coefficients with and without the magnetic field present. k_B depends on the orientation of the chamber with respect to the magnetic field and the beam axis. For the current clinical MR-linac facilities the beam is always perpendicular to the magnetic field. Therefore, ion chambers can be either oriented perpendicular or parallel to the magnetic field. Four independent methods have been developed in this project to measure ionisation chamber specific k_B correction factors:

1. A primary standards-based method. With this method ionisation chambers are directly calibrated against a primary standard in an MR-linac. This is done with the magnetic field present and repeated after ramp down of the magnetic field. Ion chambers were calibrated both perpendicular and parallel to the magnetic field[4].
2. An indirect method. With this method the calibration coefficient of an ionisation chamber at zero magnetic field is determined at NPL as a function of $TPR_{20/10}$ and interpolated to the value measured in an MR-linac. The calibration coefficient in the presence of magnetic field (i.e. directly in an MR-linac) is obtained using alanine as a transfer standard. The effect of the magnetic field on alanine response (figure 2) is taken into account and corrected for in the transfer.
3. A method based on a combination of an electromagnet and a conventional linear accelerator (see Figure 4). With this method ionisation chambers are placed between the poles of the electromagnet. The ion chambers are irradiated with a beam with a similar quality as for MR-linacs. The magnet is ramped up in steps from 0 T to a maximum magnetic field strength. At each step the charge collected by the ion chamber, M , is measured. The change in D_w at the point of measurement is calculated by means of Monte Carlo simulations or by using alanine as transfer standard. This dataset is used to generate k_B factors for each magnetic field strength (see for example Figure 3 c). Since the space between the electromagnet poles is limited only the perpendicular orientation between chamber axis and magnetic field can be used in these facilities [7].

4. Method based on chamber monitor ratio in MR-linac facility. This method uses a monitor positioned outside the magnetic field of the MR-linac to monitor the beam output. The ionization chamber is positioned inside the MR-linac. The change in D_w at the point of measurement is calculated by means of Monte Carlo simulations. From this data, the k_B of the chamber can be determined for the MR-linac beam and for different orientations [3].

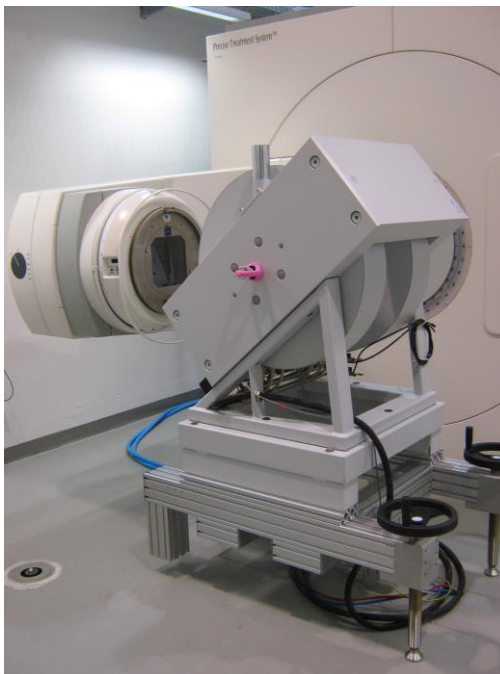


Figure 4 The PTB Facility to determine k_B factors by the combination of an electromagnet and a conventional linear accelerator.

Type specific correction factors for ionization chambers can only be applied if the intra-type variability is sufficiently low. Therefore, additional investigations have been carried out in the project to determine the variation in k_B among chamber of the same type [8]. This was done for the different orientations (parallel and perpendicular) and for two commonly used ionisation chambers for reference dosimetry using 12 and 13 chambers in the two sets. It was demonstrated that this intra-type variability was within 0.2% for the investigated chamber types, which is sufficient for application of type specific k_B correction factors.

Table 2 k_B data measured within the project for two types of ionisation chambers (cw = clockwise, ccw = counterclockwise).

Reference	chamber axis \perp B (cw)		chamber axis \perp B (ccw)		chamber axis \parallel B (parallel)		chamber axis \parallel B (antiparallel)	
Spindeldreier2017	0.9590	0.31%	0.9540	0.31%	0.9920	0.30%	0.9930	0.30%
Pojtinger2018			0.9535	0.15%			0.9963	0.16%
Pojtinger2018		0.34%						
Malkov2018					0.9881	0.10%		
vanAsselen2018				0.21%				0.20%
vanAsselen2018			0.9630	0.21%			0.9920	0.20%
dePrez2019			0.9630	0.34%			0.9850	0.34%
Pojtinger2019		0.10%		0.01%				
Pojtinger2019		0.16%		0.16%				
NPL EMPIR			0.9580	0.20%	0.9890	0.20%	0.9890	0.20%

NPL EMPIR			0.9640	0.34%	0.9950	0.34%	
NPL EMPIR			0.9570	0.59%	0.9950	0.59%	
NPL EMPIR			0.9620	0.11%	0.9890	0.11%	0.9890 0.11%
NPL EMPIR			0.9580	0.32%			
NPL EMPIR	0.9610	0.32%	0.9630	0.32%			
NPL EMPIR	0.9550	0.11%	0.9590	0.11%			
NPL EMPIR	0.9570	0.11%	0.9640	0.11%			

Apart from the k_B correction factor also a k_Q correction factor is needed for reference dosimetry, which corrects for the change in calibration coefficient between the beam quality in which the chamber was calibrated and the beam in which the chamber will be applied. It should be mentioned that this factor holds for the situation without magnetic field present. This k_Q data is available in existing CoPs as a parameterised function of the beam quality specifier. Due to the attenuation of the MRI bore, the radiation field of MR-linac facilities differs from conventional linac fields. Therefore, k_Q factors have been determined in an MR-linac without the magnetic field present using the water calorimeter. It was shown that the determined k_Q and the associated beam quality matches well with the parametrized functions in existing CoPs.

Summary of Key-outputs

The key output of this project for the objective of a metrological framework for traceable dosimetry under reference conditions for MRgRT is the following:

1. Ionisation chambers calibrated against a primary standard with an uncertainty less than 1.2 % ($k = 2$) allow for accurate reference dosimetry which was used in the preparation of the first clinical treatments with an MR-linac
2. Formalism and methodology for reference dosimetry in MRgRT applied in preparation of first clinical treatments
3. Secondary dosimetry methods such as alanine and Fricke solutions have been characterised for application in the presence of magnetic field
4. Consistent data-set of measured chamber-type specific k_B factors, in depth characterisation of the dead volume effect for ion chambers and data on recombination and polarity effect for dosimetry in the presence of magnetic fields allows for preparing a Code of Practice for reference dosimetry in MRgRT facilities.

4.2 Measurement of treatment planning system (TPS) input data for MRgRT

Relevance

Dose calculation algorithms in commercial Treatment planning systems (TPS) rely heavily on the accuracy of the underlying beam model and of the measured dosimetrical input data that is fed into this beam model. A typical set of input data consists on depth-dose profiles, transversal profiles and output factor measurements. For conventional radiotherapy well-established procedures, methods and well characterised detectors are available. For MRgRT these measurements must be performed in the presence of magnetic fields. Therefore, the characteristics of detectors (generally these are different detectors than the secondary standards used for reference dosimetry) used for these type measurements have been investigated for application in the presence of a magnetic field. In addition, several radiation field characteristics are affected by the magnetic field. Therefore, the change of these characteristics with magnetic field strength was also investigated.

Radiation field characteristics

In this project different facilities have been used for the investigation: two clinical MR-linacs and one experimental facility that combines an electromagnet with a linear accelerator (Figure 5). A comprehensive list of beam data measurements has been made for the clinical MR-linac in conjunction with Elekta. This list has become part of the standard beam data collection set and requirements and has been published [9]. The dataset consists of the following measured radiation field characteristics:

- Output factors
- Lateral dose profiles
- Depth dose profiles
- Out-of-field doses

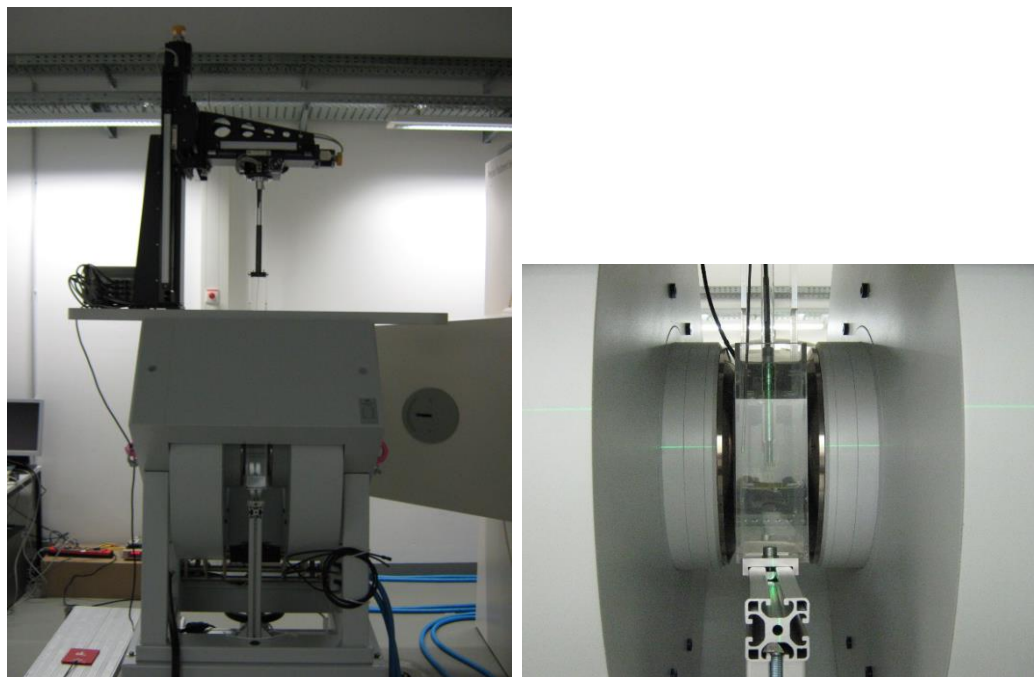


Figure 5 Pictures of PTB setup for relative dosimetry in the experimental facility consisting of a linear accelerator and an electromagnet. The positioning mechanism (top left picture) allows positioning in the electromagnet along the $xyz\phi$ -coordinate system.

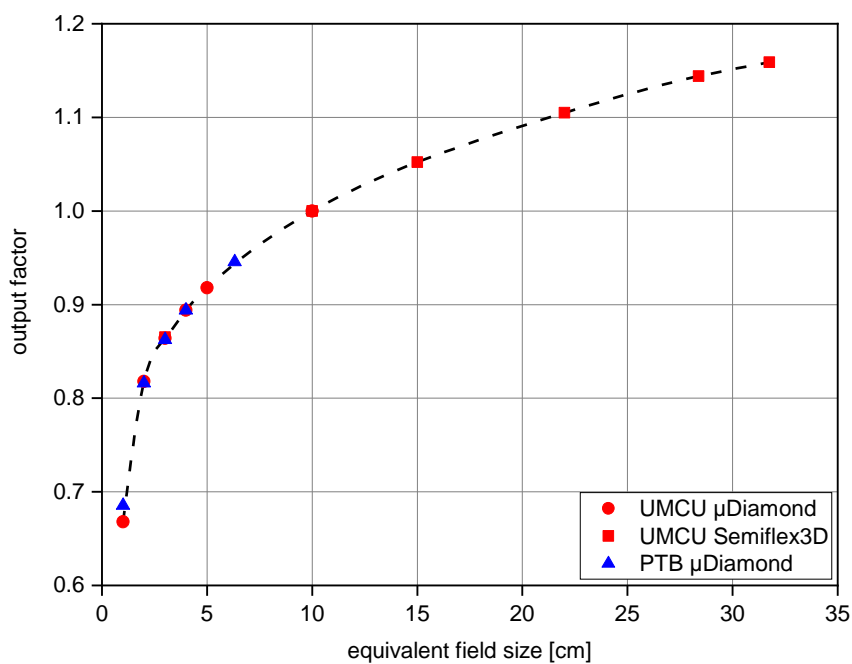


Figure 6 Comparison of output factor measurements in the experimental setup of PTB and the MR-linac facility at UMCU.

Output factors

An important aspect is the question to which extent the experimental facility mimics the clinical facilities. For this purpose, the output factors measured at the PTB facility have been compared with the data measured in a clinical MR-linac at UMCU [9]. For both measurements the same detector was used.

The comparison (Figure 6) shows an excellent agreement between both datasets, which suggests that the experimental facility simulates a clinical facility quite well. It should be noted that data for larger field size of the experimental facility cannot be compared due the field size limited by the pole gaps of the electromagnet.

From the measured output factors in the clinical MR-linac facility [9] differences between detectors have been observed for field sizes smaller than 2.0 cm. This is an indication that relative output factors (which is here a ratio of readings) are inadequate for measurement of the real output factor (a ratio of dose) for small fields. From this it can be concluded that detector specific correction factors for small dosimetry in MRgRT facilities are needed.

Lateral dose profiles

Lateral dose profiles have been measured for a range of magnetic field strengths, field sizes and beam qualities in the experimental setup. From these profiles the change in penumbra size as a function of magnetic field strength was investigated (see for example Figure 7). From this data set it can be concluded that the maximum change in penumbra size is 0.8 mm.

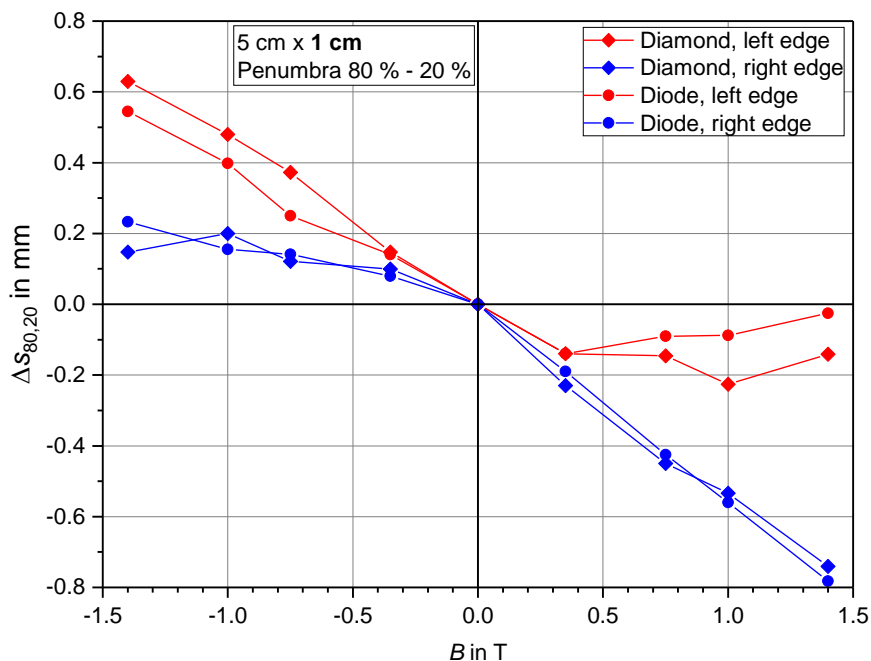


Figure 7 Change of penumbra size as a function of magnetic field strength, measured with two different detectors, (Diamond and diode) and for two sides of the lateral dose profile.

Depth dose profiles

Depth dose profiles have been measured for two beam qualities (6 and 8 MV) and for magnetic field strengths between 0 and 1.4 T. From these beam profiles the change in position of dose maximum D_{max} was derived. It was shown that the maximum shift in position of D_{max} was more than 5.0 mm. In addition, it was discovered that the shift of the D_{max} positions is not a monotonous increase with magnetic field strength. Instead the shift for field strengths lower than 0.4 T is in the opposite direction. This is especially relevant for MR-linacs using a 0.35 T MRI system.

At the exit of the water phantom a dedicated thin window was used to be able to measure the dose-build-up due to the electron return effect. This was done as function of the magnetic field strength. The results of these measurements are shown in Figure 8.

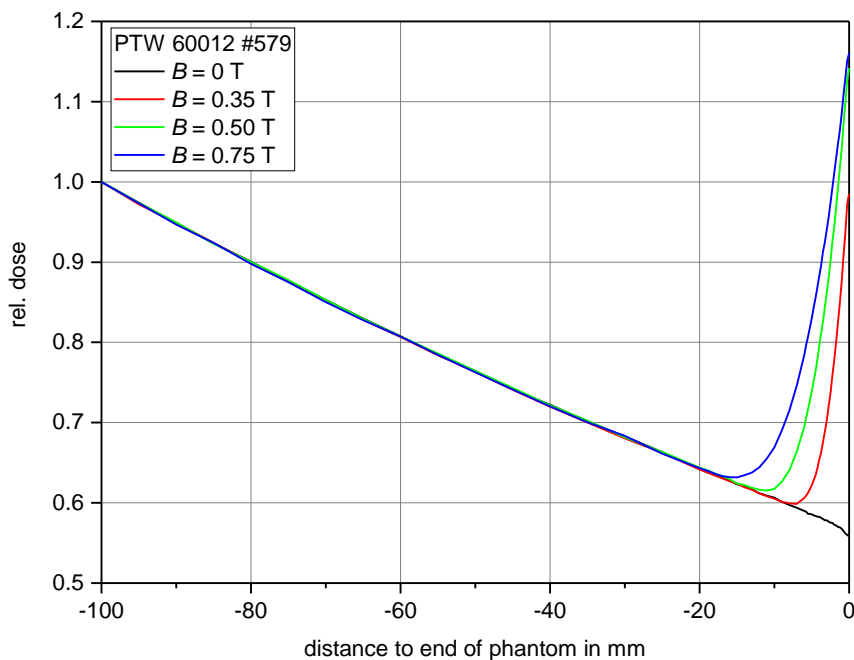


Figure 8 Depth dose profile at exit of water phantom for different magnetic field strengths.

Out-of-field dose

To investigate the effect of magnetic fields on out-of-field dose, Monte Carlo studies have been conducted. Two different sources of out-of-field doses have been considered:

1. Contaminant electrons generated in air or in the MR-linac bore crossed by the beam [10]
2. Electrons back-scattered from the phantom [11]

It was shown that the contribution from contaminant electrons is small (< 5 %), However, out-of-field doses from back scattered electrons can be large (> 30 %) and should be considered by dose algorithms of TPS.

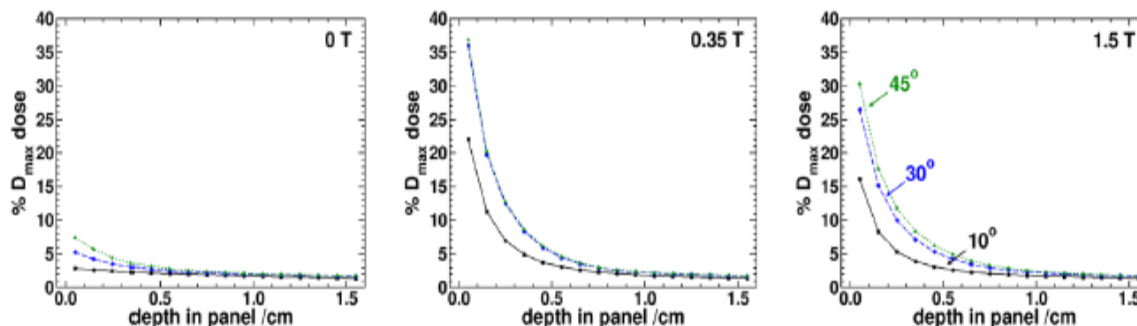


Figure 9 Depth dose curves for the exit simulation with a 10, 30 or 45° incline for 0, 0.35, and 1.5 T. Reproduced from [11] with permission.

Dose mapping

Two dose mapping techniques have been investigated in this project: a 2D method based on radio chromic film dosimetry and a 3D method based on Fricke dosimetry. In this project the stability of the Fricke gel over time was optimized and the influence of oxygen concentration on the reproducibility was investigated. To lower the gel read-out signal to noise ratio, the gel composition and the MRI sequence parameters have been optimized. The global uncertainty on the dose delivered to the tumour is 7% ($k=1$) for a dose of approximately 20 Gy, with a detection limit of about 0.7 Gy. For relative dose distribution measurements, the uncertainty amounts 4% ($k=1$) for a dose delivered of approximately 20 Gy. The establishment of several calibration curves in different magnetic fields (0 T, 0.4 T, 1 T, 1.5 T) at UMCU, has shown no significant dependency of the response to the strength of the magnetic field (see Figure 10).

Measurements have been done to see if the presence of a magnetic field during irradiation has an impact on the calibration coefficient of the gel. Gel vials have been irradiated in a UMCU electromagnet, with field strength ranging from 0 T to 1.5 T and read out with the Philipps MRI 1.5 T imager embedded in the Elekta Unity 2, using a larger antero-posterior coil. Uncertainties thus obtained are larger than those expected from the optimization of the dosimetry method. It is expected to be due to the coil used, while the most accurate results were obtained using a head coil.

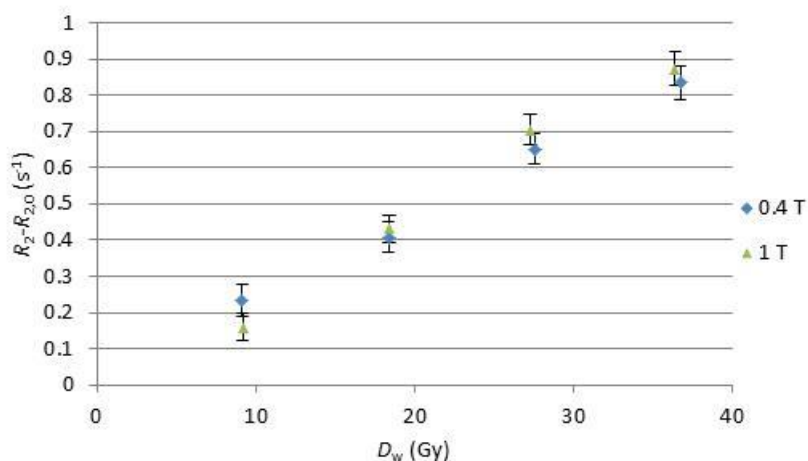


Figure 10 Dependency Fricke gel calibration curves on magnetic field strength. Readings with Elekta Unity 2 MRI, in terms of transverse relaxation rate R_2 . The variation of relaxation rate $R_2 - R_{2,0}$ due to the absorbed dose to water has been studied.

The influence of the magnetic field on the response of radio chromic films was investigated [12]. It has been demonstrated that there is small effect of the magnetic field on the response and therefore radio chromic film is considered a suitable method for dose mapping in MRgRT.

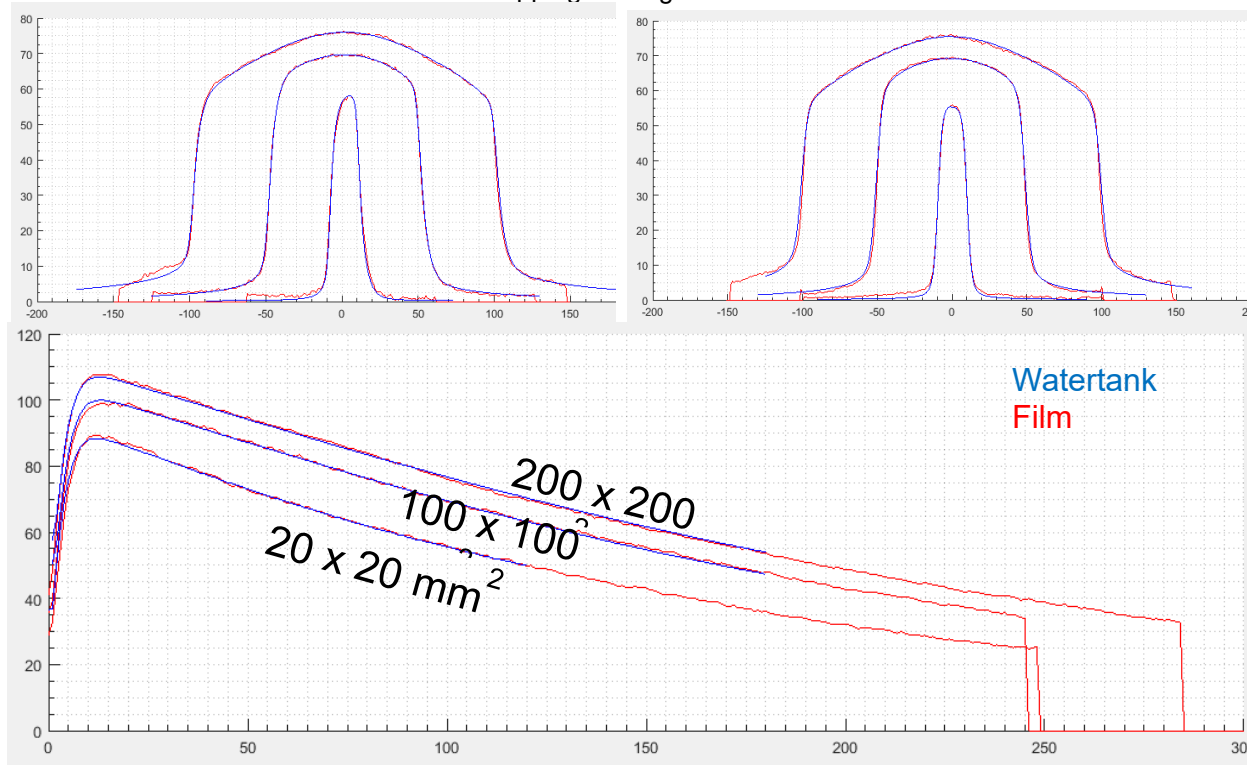


Figure 11 Beam data set based on film compared with water tank measurements

Dose mapping in an MR-linac using conventional water tank measurements is complicated in practice, because alignment tools available in conventional RT facilities (such as lasers and light field) are not available in MR-linac facilities. Instead a film-based method has been developed, which uses a series of stacked films in a solid phantom to measure the 2.5 D dose distribution in a single measurement. Alignment can be done based on the alignment tools available in the MR-linac. This approach has the advantage of a high spatial resolution measured over a larger volume than for water tank measurements. To validate the developed approach the measurements have been verified against water tank measurements. It can be seen from the excellent agreement between both measurements (Figure 11), that the film based is an adequate solution for dose mapping in MRgRT. Beam data input for the TPS of the MR-linac was measured, and a beam model has been created based on this data set. This beam model was used in the first patient treatments with the MR linac in the FIM study.

To compare both dose mapping methods investigated in this project (Fricke gel and radio chromic film) profile measurements in reference conditions 10x10 cm² fields have been done in the Elekta Unity MR-Linac at UMCU using both techniques. Although the results are compatible, film dosimetry remains the most suitable dosimeter, over Fricke gel dosimeters, for 2D dosimetry for machine quality control.

Characteristics of chambers for relative dosimetry

For relative dosimetry in general other detectors with a smaller sensitive volume are used than for reference dosimetry. For these detectors their response dependency on the magnetic field was investigated in a similar way as for the ion chambers used for reference dosimetry (see Figure 3). An example of these investigations is shown in Figure 12. It is observed that this type of detectors shows a much larger asymmetry in the response curve. Furthermore, the intra-type variation for these detectors in general is higher than for reference type ionisation chambers.

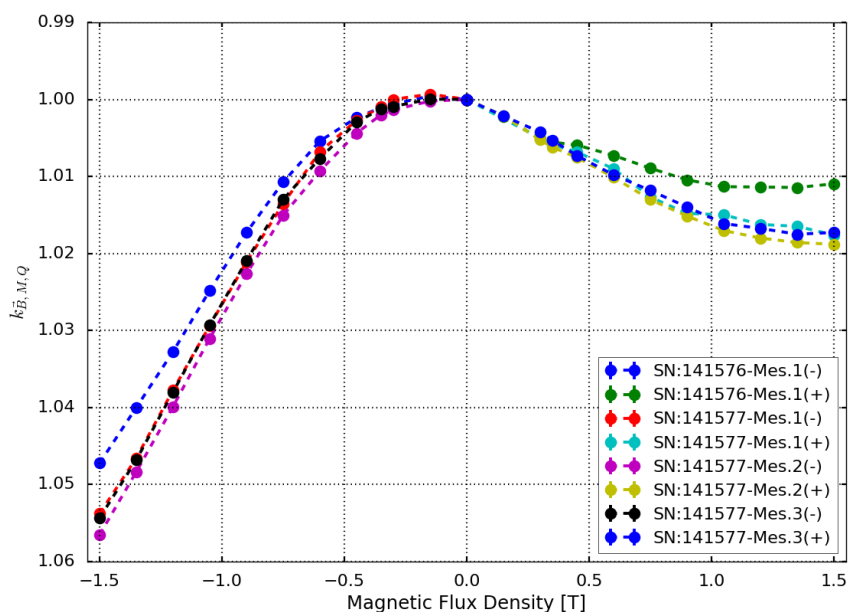


Figure 12. Response change of a PTW 31021 ionisation chamber for relative dosimetry as a function of magnetic field strength.

Monte Carlo simulations of small ion chambers in a conventional 6MV linac beam for various magnetic field strengths and orientations showed increased sensitivity of ion chamber response (especially for mini- and micro-ion chambers) due to details of chamber geometry including dead-volume effects. Lack of precise information about actual chamber dimensions may explain the less good agreement between Monte Carlo simulation and measurements. The discrepancy was up to 1.8% for Semiflex chambers, but up to 3.9% for PinPoint chambers.

The angular sensitivity of the micro diamond detector has been investigated with and without magnetic field ($B = 1.5$ T) it was shown that the angular sensitivity increases considerable with the magnetic field [9]. Characteristics of many other detectors (Small ion chambers, diodes) have been investigated as well. From

these characteristics a list has been drafted which indicates which detector can be used for a certain type of measurement.

Summary of Key-outputs

1. Film based approach can replace conventional water tank measurements for commissioning MR-linac TPS.
2. Detector specific correction factors for small field dosimetry in MRgRT facilities (field size < 2.0 cm) are needed.
3. Detailed analysis of radiation field characteristics as a function of magnetic field strength
4. Evidence that experimental facilities can be used to mimic clinical MR-linacs
5. A comprehensive list of beam data measurements for the clinical MR-linac has become part of the standard beam data collection set and requirements.

4.3 Accuracy of the Monte Carlo based radiation transport in magnetic fields

Relevance

Monte Carlo simulations of radiation transport have been used since the 1990's to simulate the response of ionisation chambers in radiotherapy applications. With the increased accuracy of Monte Carlo codes this led to an increased consistency between Monte Carlo simulated and measured k_Q correction factors. Monte Carlo simulations of radiation transport in the presence of magnetic field requires that the Lorentz force acting on the charge particle is implemented in the Monte Carlo code. Three of the most used Monte Carlo algorithms for this type of simulations: EGSnrc, PENELOPE and Geant4 have implemented the Lorentz force. Depending on the implementation one or more simulation parameters steers the accuracy of the simulation of radiation transport in magnetic fields. The accuracy of these codes for detector response simulations in the presence of magnetic fields and its dependence on these simulation parameters has been poorly investigated due to the lack of both theoretical and experimental benchmark methods. Only very recently a test to benchmark (the so-called Fano test) this accuracy by theoretical means was developed. This test was applied to three of the most commonly used Monte Carlo algorithms for detector response simulations. Furthermore, facilities for experimental benchmarking of these simulations didn't exist and have been developed and optimized in this project.

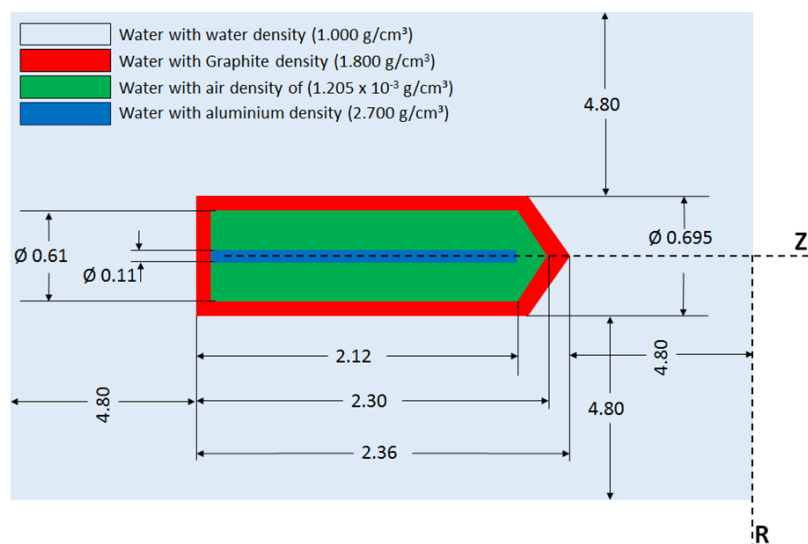


Figure 13 Consensus simulation chamber geometry for Fano test.

Fano tests

As part of this project a Fano test was designed to assess the accuracy of the three aforementioned Monte Carlo codes. This Fano test uses a consensus geometry of an ionisation chamber which is close to the geometry of real ionisation chambers (see Figure 13). This geometry was discussed and agreed by all the

involved partners. The test was performed for at least two spectra of the radiation field which were generated for a 6 MV and 8 MV linac beam. The test was performed for at least two magnetic field strengths; 0.0 T and 1.5 T. Furthermore, the test was used to investigate which settings of simulation parameters are needed to yield accurate results for all three Monte Carlo codes.

Table 3 Results of the Fano test for EGSnrc using the 6 MV spectrum. Normalised dose for cavity materials of different water density for a perpendicular orientation of the magnetic field ($B=0, 0.35$ & $1.5T$ with the simulation parameters EM ESTEPE=0.01 and ESTEPE=0.25), with their type A standard uncertainties ($k=1$) are shown.

	0T		0.35T		1.5T	
	Norm dose	Uncert	Norm dose	Uncert	Norm dose	Uncert
air	1.0001	0.0010	0.9997	0.0009	1.0029	0.0011
water	0.9986	0.0008	1.0002	0.0008	1.0002	0.0008
graphite	0.9991	0.0009	0.9985	0.0007	1.0006	0.0007
aluminium	0.9990	0.0008	0.9997	0.0006	0.9982	0.0006

Table 4 Results of the Fano test for PENELOPE for different beam qualities and as a function of the simulation parameters a and uE for a perpendicular orientation of the magnetic field ($B = 1.5 T$) with respect to the chamber axis. Uncertainties represent the type-A standard uncertainties ($k=1$).

$E(\text{MeV})$	uE	$a = 0.2$			$a = 0.5$			$a = 1.0$		
		Q	$u(Q)$	E_n	Q	$u(Q)$	E_n	Q	$u(Q)$	E_n
0.1	1%	0.9997	0.10%	0.30	1.0006	0.10%	0.58	1.0009	0.10%	0.94
0.2	1%	0.9999	0.10%	0.05	1.0001	0.10%	0.14	1.0005	0.10%	0.53
0.5	1%	1.0002	0.10%	0.16	0.9997	0.10%	0.31	1.0002	0.10%	0.23
1.0	1%	0.9996	0.10%	0.42	0.9998	0.10%	0.22	1.0008	0.10%	0.83
2.0	1%	0.9995	0.11%	0.43	0.9999	0.11%	0.06	1.0000	0.10%	0.03
5.0	1%	0.9982	0.12%	1.43	0.9984	0.13%	1.25	0.9989	0.12%	0.88
6MV	1%	1.0001	0.11%	0.11	1.0001	0.10%	0.09	1.0006	0.10%	0.41
8MV	1%	0.9992	0.13%	0.48	0.9993	0.13%	0.39	0.9999	0.13%	0.08
0.1	5%	1.0008	0.10%	0.85	1.0014	0.10%	1.47	1.0010	0.10%	1.02
0.2	5%	1.0003	0.10%	0.33	1.0010	0.10%	0.98	1.0029	0.10%	2.92
0.5	5%	0.9992	0.10%	0.77	1.0014	0.10%	1.40	1.0026	0.10%	2.63
1.0	5%	0.9998	0.10%	0.23	1.0010	0.10%	1.00	1.0020	0.10%	1.94
2.0	5%	0.9997	0.10%	0.31	1.0008	0.11%	0.77	1.0003	0.10%	0.31
5.0	5%	0.9998	0.13%	0.15	0.9983	0.12%	1.38	0.9992	0.12%	0.69
6MV	5%	0.9993	0.10%	0.55	0.9995	0.10%	0.40	1.0011	0.10%	0.79
8MV	5%	0.9993	0.14%	0.40	1.0003	0.14%	0.18	0.9996	0.13%	0.26
0.1	10%	1.0011	0.10%	1.11	1.0002	0.10%	0.23	1.0014	0.10%	1.47
0.2	10%	1.0007	0.10%	0.72	1.0009	0.10%	0.91	1.0024	0.10%	2.40
0.5	10%	1.0008	0.10%	0.77	1.0002	0.10%	0.23	1.0020	0.10%	2.01
1.0	10%	1.0001	0.10%	0.11	1.0000	0.10%	0.04	1.0015	0.10%	1.50
2.0	10%	1.0000	0.11%	0.00	1.0001	0.11%	0.09	1.0015	0.11%	1.37
5.0	10%	0.9988	0.12%	1.01	1.0001	0.13%	0.06	0.9990	0.12%	0.79
6MV	10%	0.9992	0.10%	0.64	1.0000	0.10%	0.02	1.0018	0.10%	1.35
8MV	10%	1.0003	0.14%	0.19	1.0005	0.14%	0.33	1.0004	0.13%	0.24

A subset of the results for the Fano tests are shown in Table 3 Results of the Fano test for EGSnrc using the 6 MV spectrum. Normalised dose for cavity materials of different water density for a perpendicular orientation of the magnetic field ($B=0, 0.35$ & 1.5 T with the simulation parameters EM ESTEPE=0.01 and ESTEPE=0.25), with their type A standard uncertainties ($k=1$) are shown. Table 3 and Table 4. Overall it was concluded that all three Monte Carlo codes were able to pass the Fano test. This depends on the applied simulation parameters as well as on the orientation of the magnetic field with respect to the chambers. Therefore, it is recommended to perform a Fano test for each detector geometry and magnetic field orientation.

Experimental benchmarks

Experimental benchmarks have been developed in this project and were applied to a PTW TW30013 Farmer-type ionisation chamber. The benchmarks are based on a setup consisting of a linac or a Co-60 source with an electromagnet (see Figure 14). Using a modified water phantom, the dimensions that fit within the electromagnet pole gap, an ionisation chamber can be positioned at a reference distance and depth from the radiation source. The chambers are positioned directly in contact with water, to avoid air gaps around the chamber. Then, the charge is collected for each investigated magnetic field strength. The ratio of the charge for a magnetic field strength normalized to the charge without magnetic field is calculated for the comparison with the simulated response changes.

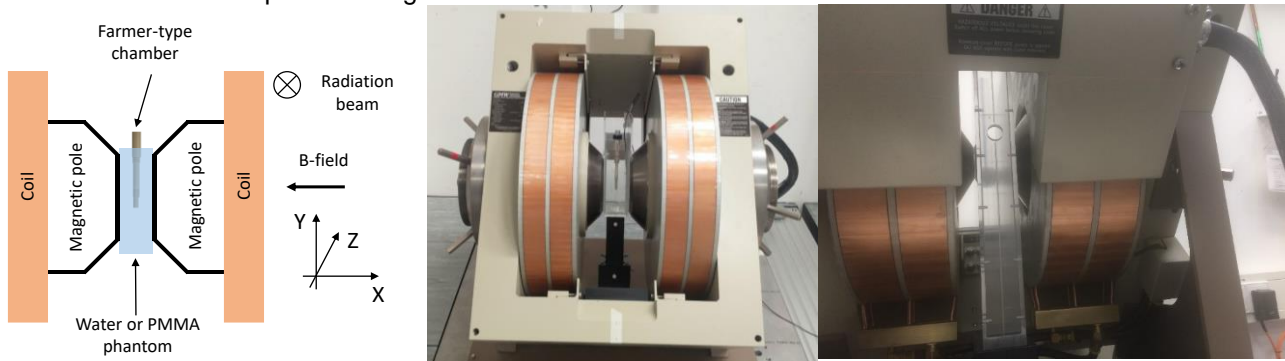


Figure 14 NPL (left and middle picture) and VSL (right picture) electromagnet setup in front of respectively a linear accelerator and a Co-60 source (not shown on the pictures).

The geometry modelled in the Monte Carlo code consists of the phantom, the ion chamber based on the manufacturer blueprints and the pole faces. The beam is modelled based on the phase space files already available of the irradiation facilities. Using this model, the energy scored in the sensitive volume (i.e. excluding the dead volume) of the ion chamber is calculated as a function of the magnetic field strength. For these simulations the simulation parameter values that gave accurate results in the Fano test were used. The response for a certain magnetic field strength is calculated as the cavity dose scored normalized to the cavity dose for $B = 0.0$ T. The calculated response is compared to the measured response. Note that since the change in dose is not considered, the calculated response change (Figure 15a) does not equal k_B factors (Figure 15 b) and serves only to benchmark the Monte Carlo codes.

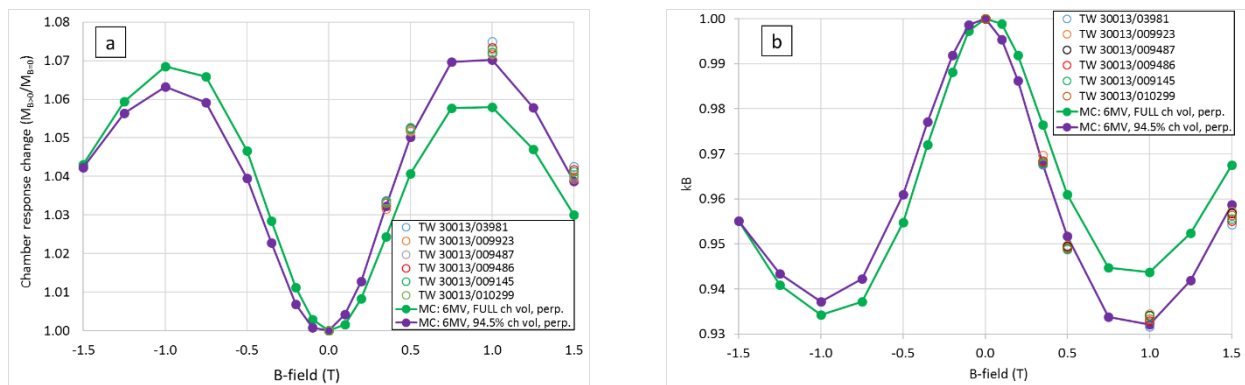


Figure 15 Results of the experimental benchmark of EGSnrc for the PTW 30013 ionisation chamber. Chamber response change (a) and k_B (b) as a function of magnetic field strength.

These experimental benchmarks have been carried out for a set of chambers of the same type to account for intra-type variability and for Co-60, 6 MV and 8 MV beam qualities. An example of the results obtained by the NPL are shown in Figure 15. From these experimental benchmarks it can be concluded that the level of agreement between measurements and simulations is in the order of 0.3 %, which for the main part can be attributed to intra-type variability of the ionisation chambers.

The key output of this project for the objective of assessment of accuracy of the Monte Carlo based radiation transport in magnetic fields is the following:

1. Three Monte Carlo pass the developed Fano test for the investigated consensus chamber geometry, for a specific set of simulation parameters within 0.6 % for GEANT4 and within 0.1% for PENELOPE and EGSnrc.
2. The developed Fano tests allows to set the simulation parameters required for accurate detector response simulations in the presence of magnetic fields
3. Experimental benchmarks show an agreement between simulations and measurements on the level of 0.3 % which can be mainly attributed to intra-type variability of the investigated ion chamber.

4.4 Evaluation of MR based dose delivery under static and dynamic conditions

Relevance

Clinical implementation of MR-guided therapy with dedicated MR-integrated radiation devices requires thorough quality assurance (QA) measures to guarantee that the dose distribution is delivered as intended in treatment planning for each treatment fraction. An important aspect here is that inter- (e.g. repositioning of the patient) and intra-fractional (e.g. breathing motion) motion has to be measured (by the MRI) and compensated for within treatment workflows. Therefore, quality assurance challenges for MRgRT requires the use of sophisticated anthropomorphic phantoms which are able to mimic motion and deformation in combination with 2D and 3D high resolution dosimetry techniques. In addition, there is a need for techniques that are able to monitor organ motion independently from the MRI in real-time. Apart from the quality assurance challenges related to organ motion, technical realisation of clinical workflows in MRgRT introduces also significant challenges on the quality assurance of the machine, such as, image contrast, isocenter alignment potential magnetic field distortions.

Therefore, in this project

- Methods for 2D- and 3D-dosimetry techniques have been characterised and further developed for application in complex clinical radiation fields;
- dedicated phantoms have been designed, constructed and commissioned;
- specific end-to-end-tests for treatment scenarios with intra- and inter-fraction motion have been developed;
- Machine quality assurance methods have been developed;
- A method for organ motion monitoring based on UWB-radar was investigated based on a simulation platform;
- A simulator has been developed to assess the residual uncertainties from organ motion for realistic clinical treatment scenarios;

2D and 3D dosimetry of clinical dose distributions

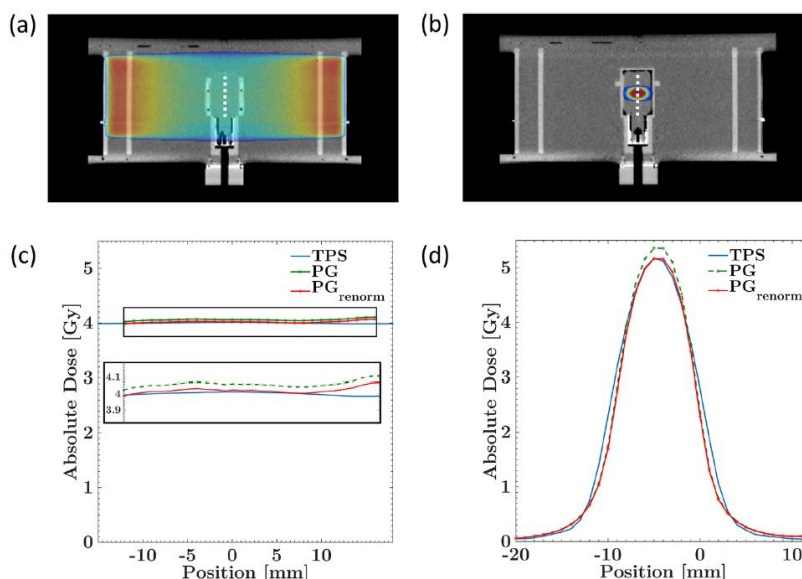


Figure 16 TLD and polymer gel results. Representative coronal slices of the calculated dose distribution for homogeneous (a) and small-field irradiations (b). The white dotted lines indicate the orientation of the dose profiles shown in (c) and (d). Calculated dose profiles (TPS, blue) are compared with (PG_{renorm} , red) and without (PG , green) renormalization. Reproduced from [13] with permission.

Considerable progress in the field of 3D-dosimetry techniques has been made in this project. Fricke and polymer gel dosimetry has been investigated. Both methods are sensitive to oxygen and other contaminations

in the gel holder. Therefore, traditionally the preferred materials for these holders are made of glass, which is considered chemically inert. To mimic clinical reality as close as possible it is highly desirable to be able to shape holders in complex shapes in a flexible way, for example to simulate the organ of a real patient.

Since 3D printing offers this flexibility and versatility, several 3D-printing materials have been investigated for their characteristics to serve as material for a gel holder. It has been shown that VeroClear™ is suited to be used as holder material for polymer gel [14].

In addition, the use of polymer gel was investigated for clinical dose distributions [13,15]. One problem of polymer gel dosimetry and most gel dosimetry techniques is to measure the 3D dose distribution in an absolute way with a low uncertainty. This mainly results from the uncertainty on the calibration curve, which must be derived from measurement with different flasks of gel. Therefore another approach has been investigated, which is the combination of TLDs with polymer gel [13]. It has been shown that this combination results in a more robust and accurate method for absolute 3D dosimetry.

Polymer gel and Fricke gel have been compared and shown to agree within the uncertainties and with calculated dose distributions.

Development of phantoms

As part of this project several phantoms have been developed and/or optimized for application in MRgRT. An overview is provided in Figure 18. These phantoms have been used in the context of machine quality assurance (phantom a), end-to-end tests for patient quality assurance (phantom b-c), and for the development of organ motion monitoring techniques based on UWB-radar.

Machine quality assurance

Phantom A was used for testing imaging and irradiation isocenter accuracy as well as image distortions in this project. The phantom is visible both on CT and MRI and was equipped with a 3D polymer dosimetry gel container which allows for 3D evaluation of “star-shot”-irradiations [16]. Using this phantom, the alignment between the MR imaging isocenter and the irradiation beam isocenter could be measured. This resulted in an alignment in three directions which was lower than 0.9 mm (± 0.9 mm) for an 0.35 T MR-linac. Furthermore, the phantom was used to determine the geometric distortion of the MR-images within 14 cm distance from the isocenter. These measurements revealed a maximum distortion of 1.4 mm and mean distortions of (0.59 ± 0.28) mm.

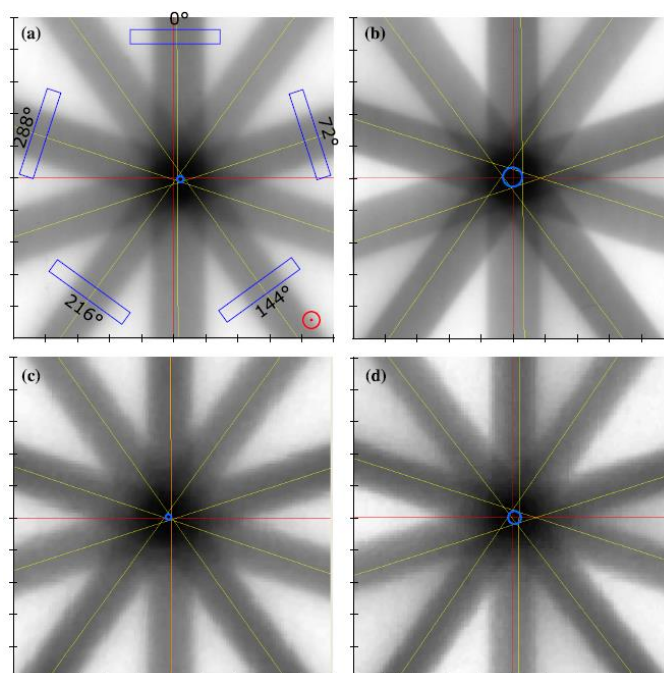


Figure 17 Evaluated films ((a) and (b)) and PG-based T2-Maps ((c) and (d)) for magnetic field strengths of 0 T ((a) and (c)) and 1 T ((b) and (d)) with reconstructed beam axes (yellow), room lasers (red) and isocircles (blue). The blue boxes in (a) are located at radial distances between 21 mm and 23 mm from the isocenter and indicate the area over which beam profiles in figure 3 were averaged. As indicated in (a), the magnetic field is oriented towards the reader. The ticks on the axes indicate 5 mm increments. Reproduced from [16] with permission.

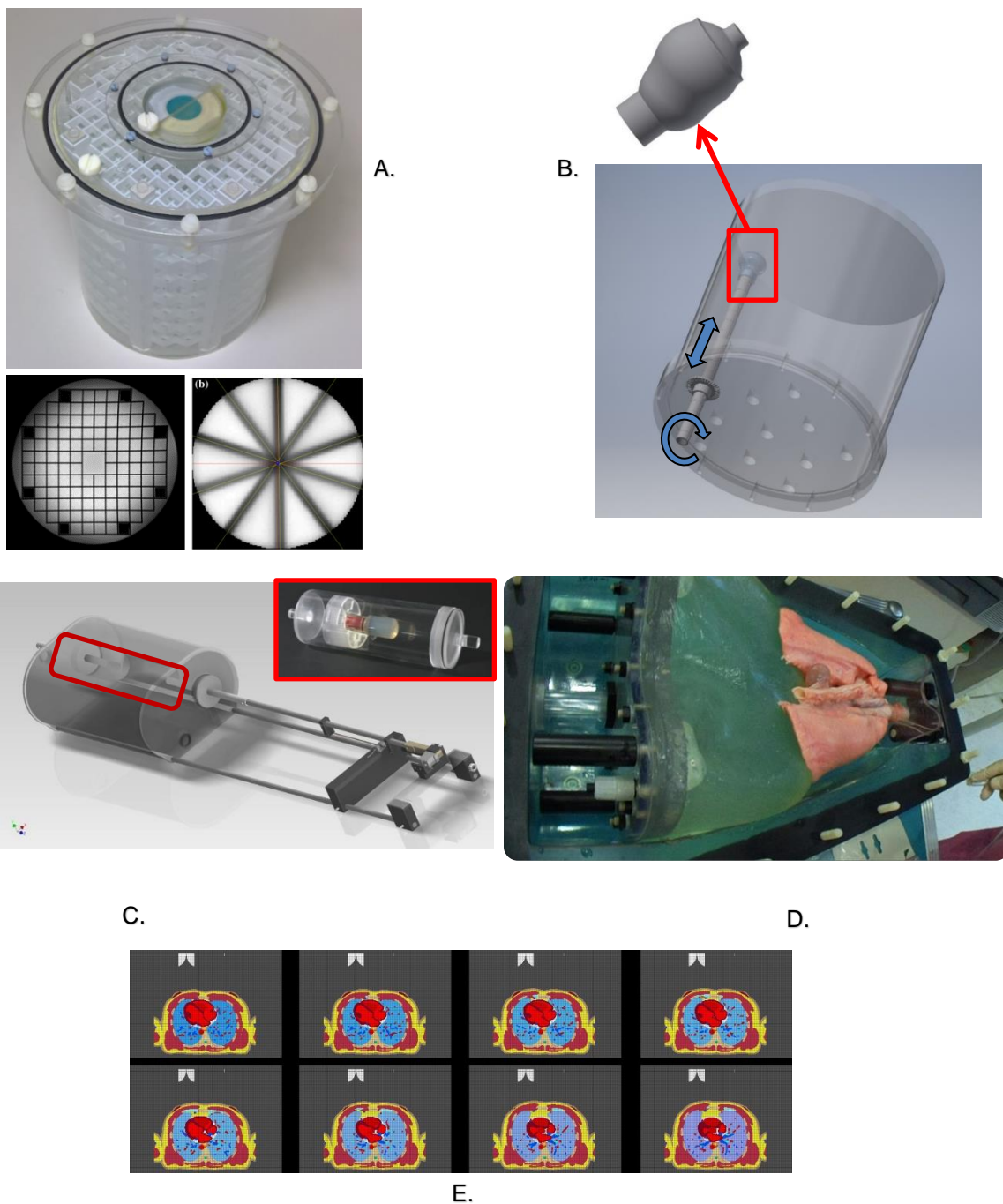


Figure 18 Overview of phantoms developed and/or optimized for application in MRgRT in this project. a. phantom for machine QA with both MRI and CT contrast which allows to determine both MRI and radiation isocenter in a single measurement and MRI image distortion in an area around the isocenter, b Quality assurance phantom which allows for reproducible inter-fractional anatomical changes, with anthropomorphic image contrast (MRI) and 3D printed gel containers. In this case a 3D printed prostate is shown, c. MRI-compatible geometrical motion phantom with a motorized moving cylinder in a water container which allows to simulate arbitrary motion patterns. Cylinders allows to insert several types of dosimeters, d. MRI-compatible anthropomorphic porcine lung phantom with artificial pneumatically driven diaphragm which allows to simulate breathing motion and to insert a gel container, e. Virtual XCAT phantom: Based on the virtual XCAT phantom 4D data sets for breathing and heart beat simulations were created and used to model 4D MRI data and UWB radar signals.

Table 5 B_0 homogeneity for different gantry angles expressed in ppm relative to the resonance frequency.

Gantry Angle	0	30	60	90	120	150	180	210	240	270	300	330
ViewRay	2.49	4.85	6.39	3.47	3.24	1.7	3.11	1.66	2.81	3.62	1.94	5.17
Elekta (U02)	0.26	0.25	0.25	0.27	0.26	0.27	0.27	0.26	0.28	0.26	0.26	0.26

A critical parameter in the geometrical accuracy of the MRI is the homogeneity of the B_0 field of the MRI scanner. This homogeneity also depends on the presence and location of large (metallic) objects, such as the MR-linac gantry.

For the 0.35 T MR-linac, a dedicated water phantom was used to quantify the B_0 homogeneities. As the Linac components are not symmetrically arranged around the MR scanner, B_0 -homogeneity was measured at different gantry angles. A standard Free Induction Decay (FID) was recorded and consecutively analysed and the peak width was extracted in parts per million (ppm) relative to the resonance frequency (see Table 5).

To measure the system B_0 homogeneity of the 1.5 T MR-linac, B_0 field maps of a 40 cm cylindrical phantom in transverse, sagittal, and coronal orientation were generated at gantry angle = 0° . To assess the additive effect of the gantry, B_0 maps were acquired from the same phantom in transverse orientation for gantry angles between 0° and 360° degrees with 30° intervals. Based on these scans a correction has been developed to correct for the influence of gantry position (as represented by its angle) on the B_0 field homogeneity. For both MR-linacs, the measured homogeneity was essentially within the vendor specifications.

End-to-end test of inter-fraction adaptive treatment workflows

Using polymer gel and phantom B from Figure 18 the first end-to-end test for MRgRT treatments workflows with inter-fraction motion was developed. The end-to-end test simulates the complete workflow including the validation of image registration [17], treatment plan adaption and dose delivery. For this the phantom was irradiated with a prescribed dose of 4 Gy to the target under three different conditions: (i) the phantom being in reference setting, (ii) in displaced setting without adapting the treatment plan and (iii) in displaced setting with online adaption of the treatment plan. Qualitative evaluation revealed that the deformable image registration algorithm was able to deform the planning MRI of the phantom in the reference setting to the online MRI of the displaced setting. All shifted and rotated structures were accurately matched, and no artefacts were found in the deformed images. While all dose constraints were met for the reference setting (i), application of the same plan for the displaced setting (ii) lead to a clear under-dosage of the tumour and an overdosage in the organs at risk. Applying the adapted plan in the displaced setting (iii), the dose distribution was restored and the dose constraints in the tumour were met. In addition, the over-dosage in the organs at risk was reduced again. Dosimetric validation for both tumour and organs at risk was realized with polymer gel. Results show very good agreement with the calculated data which is also reflected by high 3D gamma passing rates of >93 %. As a result, a successful end-to-end test for an online adaptive treatment was performed at a clinical MR-linac.

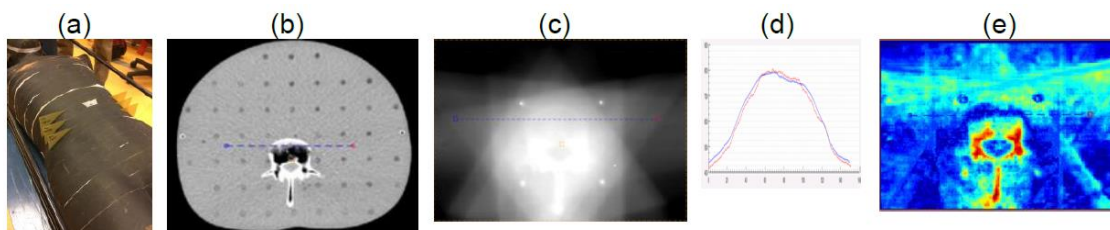


Figure 19 (a) Alderson phantom with axially inserted films. (b) a single slice of the Pseudo CT generated at the Elekta Unity MR-Linac used during the clinical workflow. (c) Processed film-based dose image. (d) Profile (dashed line in b and c) through the film (red) and TPS (blue) dose. (e) Gamma distribution of the comparison between film and TPS dose using a criterion of 3%/3mm.

To validate the full clinical workflow, an independent end-to-end test has been developed and performed during the FIM-clinical-study [2] and during clinical introduction of the CE-labelled Elekta Unity MR-linac. The end-to-end test made use of the Alderson RANDO phantom (Radiology Support Devices, CA, USA), which showed contrast in MRI (Figure 19). A film was inserted axially between two phantom slabs close to the intended target region. As the Alderson phantom contains inserts for TLDs, a few centres of these TLD-inserts were manually marked on the film. The corresponding centres in the planning MRI scan were then used to transfer the isocenter location of the MR-linac to the film. Subsequently, the clinical workflow has been performed and the plan was delivered to the Alderson phantom and the dose distribution was measured by the inserted film. The

film was processed as described in deliverable report D6 for the regular patient specific plan QA. The film-based 2D-dose distribution was registered to the 3D TPS dose distribution and the resulting translations were used as a measure for the accuracy of the MRI-linac system. The obtained translations turned-out to be less than 1 mm in all three directions.

End-to-end test of intra-fraction adaptive treatment workflow

Workflow verification for intra-fraction organ motion was realized with two previously developed phantoms (phantom C and D from Figure 18), using polymer gel and radio chromic film as dosimeters. For phantom C irradiation was carried out in static and dynamic mode with and without gating. While the agreement between calculation and measurement was very good for the static case (gamma passing rates >99 % for both film and polymer gel), a significant dose smearing with low gamma passing rates (<66%) was measured for the dynamic case. However, the initial dose distribution could be restored by gated beam delivery while the phantom was moving. This is reflected by very high gamma passing rates of >98%.

For phantom D a polymer gel container was sewed into the porcine lung. By means of an artificial pneumatically driven diaphragm, the lung could be ventilated periodically, which resulted in a significant motion of the container of >2 cm. During this motion, a gated treatment was delivered resulting in a homogeneous dose distribution in the polymer gel, while the dose to the heart, lung, esophagus and trachea was minimized. This is also reflected by the high gamma passing rates of >95%. As a result, a successful end-to-end test for a gated treatment was performed at a clinical MR-linac.

Magnetic field induced hot and cold spots

It was demonstrated that depending on the beam configurations of the treatment plan the occurrence of an air bubble introduces significant dose increase or reduction (hot and cold spots) around the air bubble. For this purpose, film dosimetry has been used to measure the dose distributions around air bubbles in a magnetic field (Figure 20). The agreement with calculations from clinical TPS gives confidence that in the situation when air pockets occur in the patients, the treatment planning system predicts the dose distributions correctly and that MRgRT treatments can be delivered safely.

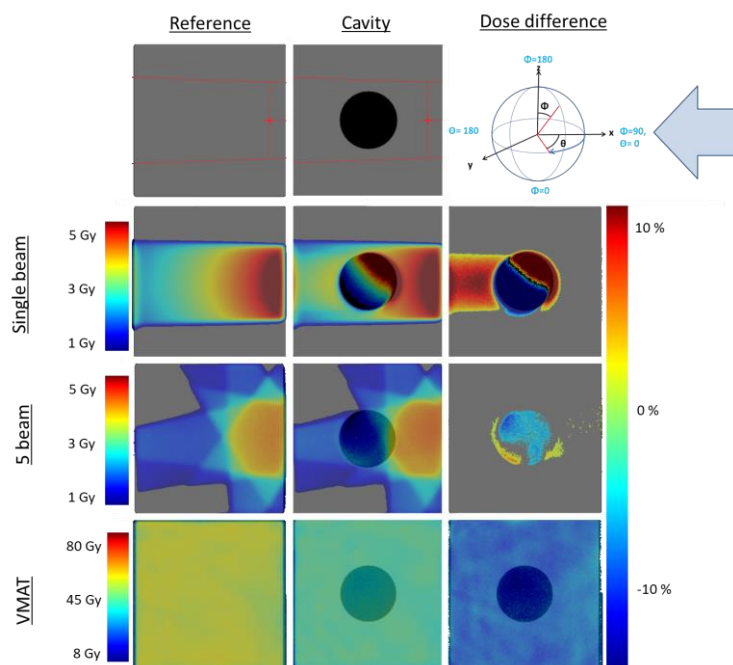


Figure 20 Magnetic field induced cold and hot spots around air cavity for a single beam and a five-beam configuration with $B = 1.5\text{ T}$ and for a VMAT configuration with $B = 0.0\text{ T}$.

Evaluation of intra- and inter-fraction organ and target motion

Since organ and target motion in radiotherapy in combination with treatment adaptation is a complex process, a simulator was developed to evaluate the impact of intra- and inter-fraction organ motion. This simulator allows to mimic several treatment scenarios and evaluate their residual uncertainties. It can be used for educational purposes. The simulator is publicly available via the [project website](#). A screenshot is shown in Figure 21.

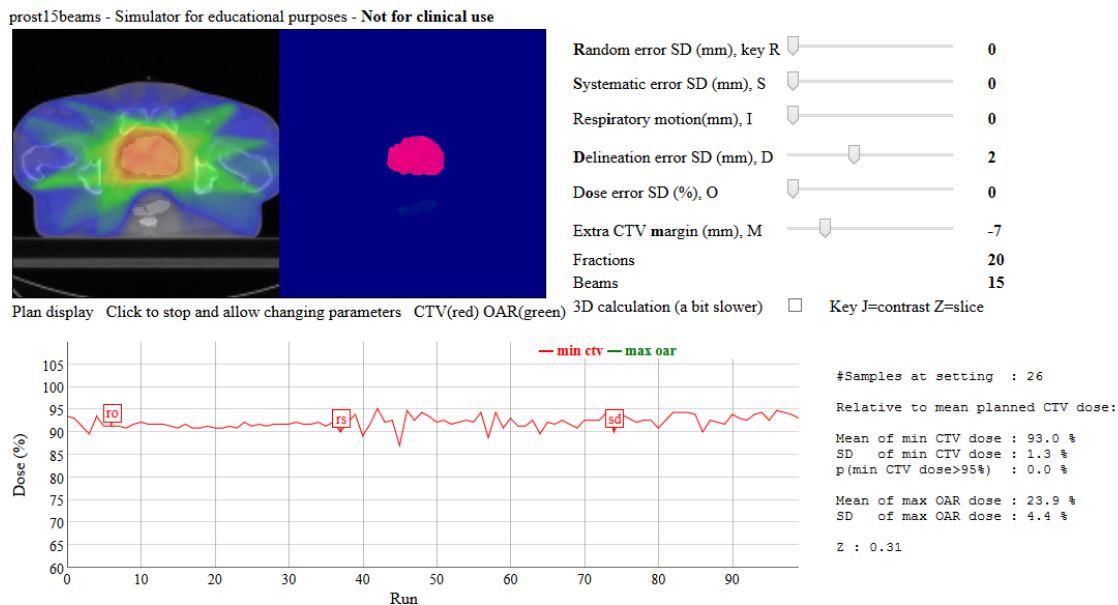


Figure 21 Screenshot of the simulator to calculate residual uncertainties from realistic MRgRT treatments.

Measurement of intra-fraction organ and target motion

A simulation test bed has been developed to calculate motion dependent UWB RADAR data. Based on a virtual phantom (XCAT) a dataset of 96 different 3D matrixes with phantom electromagnetic properties was established from 12 different cardiac and 8 different respiration phases. From this data set both UWB-RADAR and MR reference data sets was generated to exploiting respiratory and cardiac motion data available for various scenarios. For comparisons and uncertainty evaluations ground truth motion data can be extracted from the available virtual phantom models (Figure 18 E). For validation, a dynamically deformable phantom suitable for combined MR-UWB-RADAR measurements was constructed. This is first big step in the development of UWB RADAR as independent method to track organ motion with both, high spatial and high temporal resolutions in MRgRT.

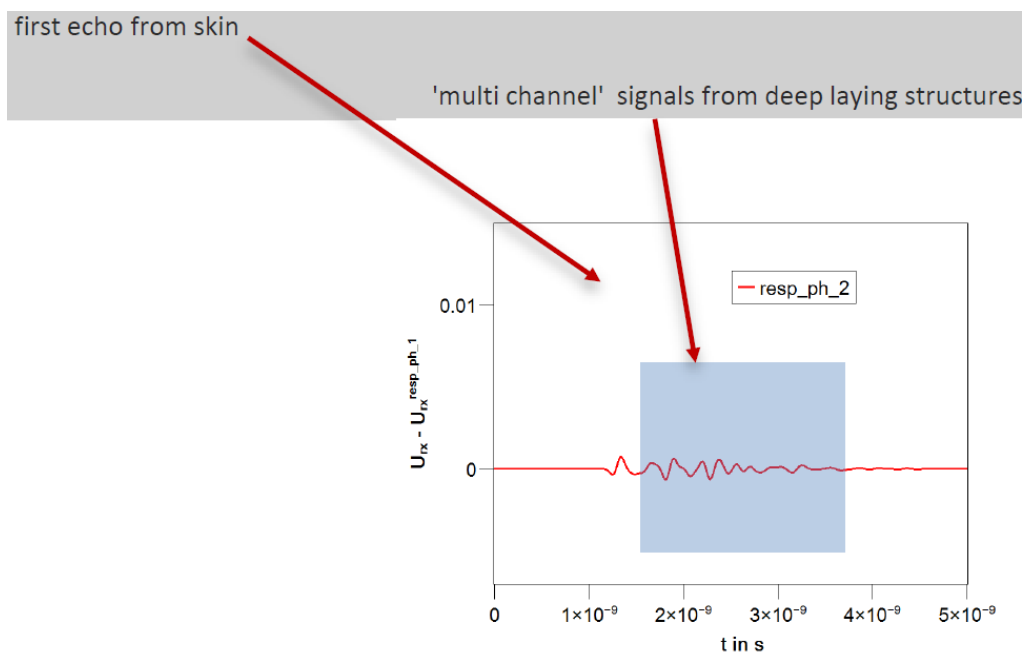


Figure 22 Simulated UWB signal based on XCAT phantom using 96 phases of the combined respiratory and cardia cycle.

The key output of this project for the objective evaluation of MR based dose delivery under static and dynamic conditions is the following:
 is the following:

1. Machine quality assurance procedures for MRgRT facilities have been developed and the performance of the facilities was demonstrated to be adequate for clinical treatments;
2. The first end-to-end tests of clinical workflows with intra-fraction motion based on sophisticated motion phantoms are available for all commercially available facilities;
3. The first end-to-end tests of clinical workflows with inter-fraction motion based on deformable phantoms are available for all commercially available facilities;
4. The magnetic field induced cold and hot spots around air cavities has been assessed and not be considered in treatment planning for MRgRT;
5. A first big step in the development of UWB RADAR as independent method to track organ motion with both, high spatial and high temporal resolutions in MRgRT has been taken based on the developed simulation test bed;
6. A simulator for educational purposes has been developed which allows clinicians to assess the residual uncertainties in clinical treatment scenarios using MRgRT.

5 Impact

The consortium has currently published 17 papers in peer-reviewed journals on an open access basis, 2 PhD thesis have been prepared and 1 MSc thesis. In addition, 85 scientific presentations on international congresses were given. The stakeholder committee consisted of 15 members from academic hospitals, medical industry and standards developing organisations. Alongside progress meetings, engagements with individual stakeholders were organised to discuss topics such as; response change of detectors in magnetic fields, machine QA of MRgRT facilities and benchmarking of Monte Carlo codes.

In June 2018, a successful satellite symposium was organised by the consortium on the topic of 'Standards and procedures for dosimetry and QA in MRgRT' with 120 attendees from 12 countries representing manufacturers, hospitals and standards developing organisations. In total, 14 presentations were given by consortium partners. The symposium covered various relevant topics (such as: reference Dosimetry for MRgRT devices, relative Dosimetry for MRgRT Treatment planning system, Monte Carlo simulations in magnetic field and QA and workflow procedures for MRgRT). In addition, the project organized several workshops such as for Monte Carlo simulations in the presence of magnetic fields, and the developed simulator.

Impact on industrial and other user communities

- hospitals and patients

The preliminary method for routine reference dosimetry at the MR-linac verified by water calorimetry in this project has been used in the clinical introduction of the MR-linac. In addition, this project has developed all elements required for a metrological infrastructure for reference dosimetry in MRgRT facilities. The preliminary method for routine reference dosimetry at the MR-linac verified by water calorimetry in this project has been used in the clinical introduction of the MR-linac. This method and other developed methods are available for clinics to assist them with reference dosimetry. Several consortium partners have assisted the commissioning of MRgRT facilities in UK, France, Germany, Denmark and Australia by performing reference dosimetry, which helped clinics in starting up the clinical treatments with MRgRT.

Clinical treatment with the MR-linac has started in May 2017 for the Unity MR-linac which is the first worldwide. Two other clinical partners started clinical MRgRT treatments afterwards. Apart from the described reference dosimetry method, several results of this project have been used in the preparation of clinical treatments, such as; methods for machine and patient QA (WP4) and characteristics of detectors used for the measurements of TPS input data (WP2). As such this project has accelerated the clinical acceptance procedures so that patients have access to a more advanced radiotherapy treatment on a shorter term. Given the interest in MRgRT facilities many more hospitals will follow. The results disseminated from this project will have a strong contribution to the clinical introduction of MRgRT in the wider community of radiotherapy clinics.

- medical devices

One commercially available MRgRT facility has achieved CE mark in 2018. Approval was based on several results of this project. To date, orders for MRgRT facilities since CE mark is higher than 50 (including already installed facilities). Therefore, the commercial expectations for the next years are high.

The existing water phantom for measurements of dose profiles as input data for TPS, has been further optimised in this project. A company who is also stakeholder in this project has started the product development and the process for commercialisation, which is expected for 2020.

The laboratory facilities for the determination of the detector's characteristics and correction factors consisting of a linear accelerator and an electromagnet, which have been developed in this project will allow manufacturers of detector and measurement equipment to characterise and calibrate their own equipment. This means that they will have commercially available detectors characterised and calibrated under stable laboratory conditions and close to clinical situations, thereby improving confidence in their equipment. As such this project has enhanced the safe introduction of (new) medical devices and measurement equipment introduced in the field of MR-guided radiotherapy. Since many new developments of measurement and QA equipment for MRgRT are to be expected for the coming years it will enhance economic and commercial activities in this field for the longer term.

Impact on the metrological and scientific communities

This project discovered the importance of the dead volume in ion chambers for measurements in the presence of magnetic field. This new discovery has been the basis for more papers on this topic which attempted to investigate the consequences for reference dosimetry and which attempted to measure the size of this dead volume more accurately.

Several fundamental concepts describe the response behaviour of ionisation chambers of which the Bragg-Gray cavity theory is the most well-known. These concepts have been shown to be essential for both the metrological community and the medical physics community in the development of standards, reference dosimetry formalisms and detector development. The investigations in this project indicate that these concepts are inadequate to describe the response behaviour of ionisation chambers in the presence of magnetic fields. The data measured in this project, to describe the response behaviour of ionisation chambers as a function of energy and magnetic field strength and orientation (WP1, WP2) will provide new information and is essential to underpin fundamental dosimetric concepts, for the description of detector response in the presence in magnetic fields, to be developed in the future.

Impact on relevant standards

A missing step is the development of a new code of practice for MRgRT. With several stakeholders (standards developing organisations (NCS, DIN, IPEM) and hospitals) the topic of reference dosimetry was discussed at the satellite symposium. The outcome of this discussion is that it is highly preferable to develop the CoP as add-on to existing CoPs. The consortium has drafted a review paper on this topic which contains an evaluation of the existing literature on this topic (which is to a large extent output of this project) and of unpublished data from this project. This review paper will be the basis for future add-ons to CoPs.

In addition, several phantoms and dosimetry techniques for QA of facilities and patient treatment have been developed in this project. With the increasing use of MRgRT the demand for QA standards increases. The developed methods from this project described in the literature will give a significant contribution to these standards. This will in the end harmonise the treatment delivery in MRgRT.

The project has contributed to the report piloted by IRSN and SFPM 'Etude sur l'installation et la mise en œuvre d'accélérateurs linéaires couplés à un système d'imagerie par résonance magnétique en radiothérapie (IRMIlinac)' (Rapport n° PSE-SANTE/2018-00007) which was drafted upon request of the ASN the France nuclear safety authority.

Longer-term economic, social and environmental impacts

After recent CE approval the number of installed and commissioned MRgRT facilities has increased rapidly. In addition, the number of new orders for these facilities remains high. The metrological basis for MRgRT dosimetry established in this project, which has also been used in the clinical introduction of MRgRT by the early adopters, will be input for future standards and CoPs. This will help clinics and manufacturers in future with the commissioning of new facilities, and as such it contributes to enhanced economic activities in this field on the long term.

In addition, with the increase in hospitals using MRgRT the number of patients that benefit from this advanced treatment also increases. Their potential benefits are:

- Reduced number of treatment fractions because accurate imaging allows for hypofractionation
- Reduced dose because of improved treatment response monitoring by MRI

- And consequently, improved quality of life and treatment outcome

In addition, via clinical trials it will be investigated whether MRgRT is a treatment option for tumour sites for which to date no treatment exist, such as pancreas. In this context the results of this project potentially contribute to the QA of these trials.

6 List of publications

- [1] Prez L De, Pooter J De, Jansen B, Woodings S, Wolthaus J. Commissioning of a water calorimeter as a primary standard for absorbed dose to water in magnetic fields Commissioning of a water calorimeter as a primary standard for absorbed dose to water in magnetic fields. *Phys Med Biol* 2019. <https://doi.org/10.1088/1361-6560/aaf975>
- [2] de Prez L, Woodings S, de Pooter J, van Asselen B, Wolthaus J, Jansen B, et al. Direct measurement of ion chamber correction factors, k_Q and k_B , in a 7 MV MRI-linac. *Phys Med Biol* 2019;64:105025. <https://doi.org/10.1088/1361-6560/ab1511>
- [3] Raaymakers BW, Jürgenliemk-Schulz IM, Bol GH, Gitzner M, Kotte ANTJTJ, van Asselen B, et al. First patients treated with a 1.5 T MRI-Linac: clinical proof of concept of a high-precision, high-field MRI guided radiotherapy treatment. *Phys Med Biol* 2017;62:L41–50. <https://doi.org/10.1088/1361-6560/aa9517>
- [4] van Asselen B, Woodings SJ, Hackett SL, van Soest TL, Kok JGM, Raaymakers BW, et al. A formalism for reference dosimetry in photon beams in the presence of a magnetic field. *Phys Med Biol* 2018;63:125008. <https://doi.org/10.1088/1361-6560/aac70e>
- [5] Pojtinger S, Dohm OS, Kapsch R-PP, Thorwarth D. Ionization chamber correction factors for MR-linacs. *Phys Med Biol* 2018;63:11NT03. <https://doi.org/10.1088/1361-6560/aac4f2>
- [6] Woodings SJ, Asselen B Van, Soest TL Van. Technical Note : Consistency of PTW30013 and FC65-G ion chamber magnetic field correction factors n.d. <https://doi.org/10.1002/mp.13623>
- [7] Spindeldreier CK, Schrenk O, Bakenecker A, Kawrakow I, Burigo L, Karger CP, et al. Radiation dosimetry in magnetic fields with Farmer-type ionization chambers: Determination of magnetic field correction factors for different magnetic field strengths and field orientations. *Phys Med Biol* 2017;62:6708–28. <https://doi.org/10.1088/1361-6560/aa7ae4>
- [8] Pojtinger S, Kapsch R-P, Dohm O, Thorwarth D. A finite element method for the determination of the relative response of ionization chambers in MR-linacs: simulation and experimental validation up to 1.5 T. *Phys Med Biol* 2019;accepted. <https://doi.org/10.1088/1361-6560/ab2837>
- [9] Malkov VN, Hackett SL, Wolthaus JWH, Raaymakers BW, van Asselen B. Monte Carlo simulations of out-of-field surface doses due to the electron streaming effect in orthogonal magnetic fields. *Phys Med Biol* 2019;64:115029. <https://doi.org/10.1088/1361-6560/ab0aa0>
- [10] Malkov VN, Hackett SL, van Asselen B, Raaymakers BW, Wolthaus JWH. Monte Carlo simulations of out-of-field skin dose due to spiralling contaminant electrons in a perpendicular magnetic field. *Med Phys* 2019;46:1467–77. <https://doi.org/10.1002/mp.13392>
- [11] Billas I, Bouchard H, Oelfke U, Duane S. The effect of magnetic field strength on the response of Gafchromic EBT-3 film. *Phys Med Biol* 2019;64:06NT03. <https://doi.org/10.1088/1361-6560/ab0503>
- [12] Mann P, Saito N, Lang C, Runz A, Johnen W, Witte M, et al. Validation of 4D dose calculation using an independent motion monitoring by the calypso tracking system and 3D polymer gel dosimetry. *J Phys Conf Ser* 2017;847:012040. <https://doi.org/10.1088/1742-6596/847/1/012040>
- [13] Mann P, Schwahofer A, Karger CP. Absolute dosimetry with polymer gels—a TLD reference system. *Phys Med Biol* 2019;64:045010. <https://doi.org/10.1088/1361-6560/aafd41>
- [14] Elter A, Dorsch S, Mann P, Runz A, Johnen W, Karger CP. Compatibility of 3D printing materials and printing techniques with PAGAT gel dosimetry. *Phys Med Biol* 2019;64:04NT02. <https://doi.org/10.1088/1361-6560/aafef0>
- [15] Dorsch S, Mann P, Lang C, Haering P, Runz A, Karger CP. Feasibility of polymer gel-based measurements of radiation isocenter accuracy in magnetic fields. *Phys Med Biol* 2018;63:aac228. <https://doi.org/10.1088/1361-6560/aac228>

- [16] Dorsch S, Mann P, Elter A, Runz A, Klüter S, Karger CP. Polymer gel-based measurements of the isocenter accuracy in an MR-LINAC. J Phys Conf Ser 2019;1305:012007.
<https://doi.org/10.1088/1742-6596/1305/1/012007>
- [17] Kraus KM, Jäkel O, Niebuhr NI, Pfaffenberger A. Generation of synthetic CT data using patient specific daily MR image data and image registration. Phys Med Biol 2017;62:1358–77.
<https://doi.org/10.1088/1361-6560/aa5200>

7 Contact details

Jacco de Pooter

e-mail: jdpooter@vsl.nl